# ARTICLES

## Magnetic Properties of Diaminoglyoxime Complexes with a Slipped-Stack Structure (2,3-Diamino-1,4-diazabuta-1,3-diene-1,4-diol)bis(2,3-diamino-4-hydroxy-1,4-diazabuta-1,3-dien-1-olato)$M^{II}$ (M = Co, Ni, and Cu)

**Takahiro Hirotsu,* Akinari Sonoda, Hirofumi Kanoh, and Kenta Ooi**

*Shikoku National Industrial Research Institute, 2217-14 Hayashi-cho, Takamatsu 761-03, Japan*

**Manabu Senô**

*Department of Industrial Chemistry, College of Science and Technology, Nihon University, 1-8 Kanda-Surugadai, Chiyoda-ku, Tokyo 101, Japan*

*Received: September 24, 1996; In Final Form: March 12, 1997*[⊗]

The magnetic properties of the divalent metal complexes [$ML_2$(HL)] (M = $Co^{II}$, $Ni^{II}$, and $Cu^{II}$; HL = 2,3-diamino-1,4-diazabuta-1,3-diene-1,4-diol, i.e., diaminoglyoxime) with a slipped-stack structure were examined. The magnetic susceptibilities and the electron spin resonance spectra indicate that [$CoL_2$(HL)] exhibits a ferromagnetic interaction along the stack chain, the strength of which is estimated to be 13.5 K, while [$CuL_2$-(HL)] is paramagnetic and [$NiL_2$(HL)] is diamagnetic. The magnetic behaviors of the [$ML_2$(HL)] complexes can be predicted precisely by comparing the spin splittings of the partially occupied molecular orbitals of the monomer complexes $ML_2$ and the dimer complexes $2ML_2$ which are equivalent in structure to the relevant moieties in the real stack chains, based on molecular calculations using the DV-Xα method. The modes of the differential spin densities for the dimers $2ML_2$ strongly suggest that the principal mechanism of superexchange on [$CoL_2$(HL)] may operate through strong interaction of the $3d_{zx}$ orbitals of Co atoms with the $2p_z$ orbitals of two apical N atoms which form the $\pi_z$-type systems of the adjacent complex molecules along the stack chain.

### Introduction

Advanced understanding of magnetostructural correlations in metal complexes has been largely derived from intensive study of molecular-based materials exhibiting spontaneous magnetization. Kahn et al. have demonstrated that the $Mn^{II}-Cu^{II}$ bimetallic chain compound with metals bridged by 2-hydroxy-1,3-propylenebis (oxamato) exhibits spontaneous magnetization at 4.6 K,[1a] on the basis of the notion that heteropolymetallic chain systems, even if the interaction between nearest neighbors is antiferromagnetic, never fail to fall into magnetic ground states owing to noncompensation of the local spins.[1b] Gatteschi et al. have found alternant $Mn^{II}$(hfac)-nitronyl nitroxide radical (NIT-R) linear chain complexes (hfac = hexafluoroacetylacetonate, NIT-R = 2-substituted 4,4,5,5-tetramethylimidazoline-1-oxyl-3-oxide; R = ethyl,[2a] *n*-propyl,[2a] and isopropyl[2b]) with spontaneous magnetization at 7.6−8.6 K by predicting the coupling of a nitronyl nitroxide directly bound to a metal ion from the overlap mode between the molecular orbitals with an unpaired electron of the ligand and the metal ion.[2c] On the basis of such a design strategy using through-bond magnetic interactions to obtain the molecular-based magnets, a two-dimensional spin network composed of $Mn^{II}$(hfac) and a trinitroxide radical having three ligating sites and a quartet ground state has already been synthesized and it exhibits a critical temperature of 3.4 K.[3] At present, the synthesis of three-dimensional oxalate-bridging networks is being explored extensively to obtain a higher critical temperature for spontaneous magnetization.[4] On the other hand, on the basis of a design strategy using through-space magnetic interactions in molecular assemblies with stacked and layered modes,[5] Miller et al. have reported that a few charge-transfer complexes such as [$Fe(C_5Me_5)_2$] (TCNE)[6a] and [$V(TCNE)_x$] [$y(CH_2Cl_2)$][6b] (Me = methyl, TCNE = tetracyanoethylene) are molecular-based magnets. Oshio et al. have described three-dimensional organic radical networks with paramagnetic metal complexes as a network component having magnetic interactions with each other through the radical network.[7] However, the mechanism of magnetic interactions between spin centers through molecular columns has not been made sufficiently clear from the molecular-orbital method. This probably makes the design of molecular-based magnets by the through-space approach difficult, but this approach is a more useful strategy, particularly for design of organomagnetic compounds,[8] rather than the through-bond approach.

We have been interested in divalent-metal complexes with diaminoglyoxime [$ML_2$(HL)] (M = Co,[9] Ni,[10] and Cu;[11] HL = 2,3-diamino-1,4-diazabuta-1,3-diene-1,4-diol, i.e., diaminoglyoxime) as a system underlying magnetic interactions in a stacked molecular chain, because these compounds are monoclinic, they belong to space group *C*2/*c*, and because their structures consist of chains of planar $M^{II}L_2$ units stacked along the *b*-axis through long M−N bonds to terminal N atoms of the adjacent molecular units; the stacked chains form sheets through hydrogen bonding with neutral HL molecules in the {002} plane for the $Co^{II}$ compound[9] and in the {201} plane for the $Ni^{II}$ [10b] and the $Cu^{II}$ compounds.[11] Recently we have found that the $Co^{II}$ compound [$CoL_2$(HL)] exhibits ferromagnetic interactions along the stack

* Author to whom correspondence should be addressed. Fax: 81-878-69-3550. E-mail: hirotsu@sniri.go.jp.

[⊗] Abstract published in *Advance ACS Abstracts,* April 15, 1997.

S1089-5647(96)02944-6 CCC: $14.00 

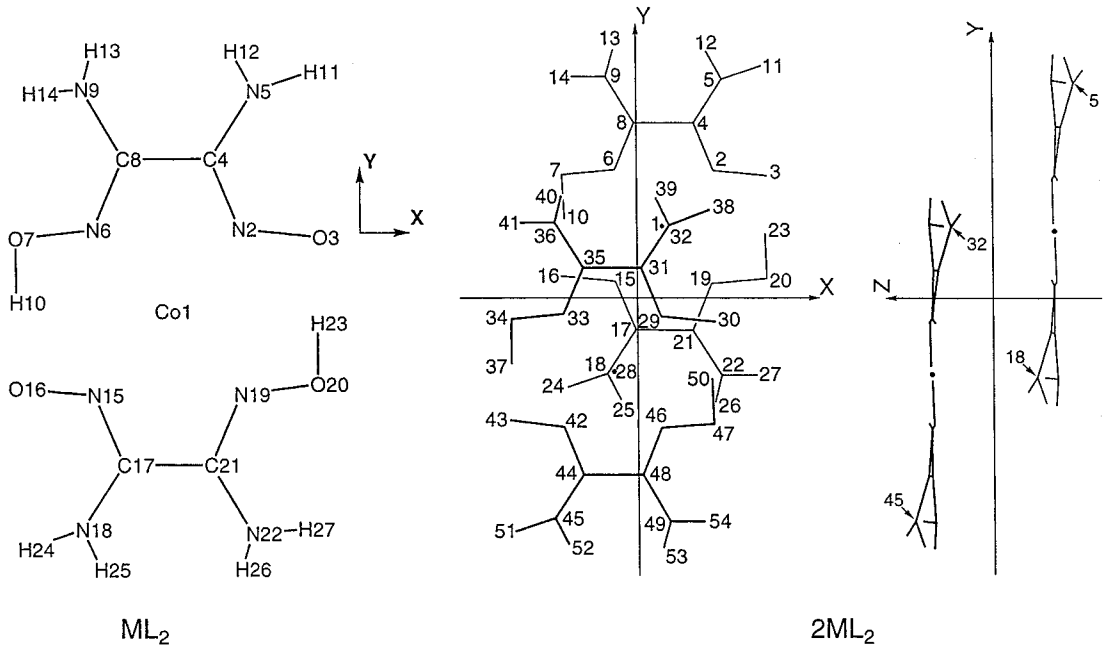


**Figure 1.** The coordinate and numbering of atoms of the monomers $ML_2$ (left) and the dimers $2ML_2$ (right). The hydrogen atoms H10 (H37) and H23 (H50) of the oxime groups are bound to the oxygen atoms O7 (O34) and O20 (O47), respectively, in the M = Co systems as in this figure and conversely, to the oxygen atoms O16 (O43) and O3 (O30), respectively, in the M = Ni or Cu systems.

chain,[12] that the $[NiL_2(HL)]$ compound is diamagnetic, and that the $[CuL_2(HL)]$ compound is paramagnetic. Both $[NiL_2(HL)]$ and $[CuL_2(HL)]$ exhibit magnetic properties quite different from that of $[CoL_2(HL)]$. In this study, we deal with the characteristic magnetic behaviors of the compounds $[ML_2(HL)]$ (M = $Co^{II}$, $Ni^{II}$, and $Cu^{II}$) in terms of their magnetic susceptibility. Also, we discuss magnetic interactions between the monomer units in the dimeric model complex $2ML_2$ with a structure equivalent to that of a pair of neighboring molecular units in the stack chain of the real system, based on molecular orbital calculations using the unrestricted DV-Xα method,[13] in order to throw light on the nature of magnetism of the stack chain of $[ML_2(HL)]$.

## Experimental Section

**Materials.** Diaminoglyoxime (HL) was obtained as colorless pillar-shaped crystals by reacting 0.1 mol of dithiooxamide with 0.2 mol of hydroxylamine in 350 mL of methanol under reflux followed by recrystallization from water with activated carbon for decoloration.[14] Anal. Calcd for $C_2H_6N_4O_2$: C, 20.34; H, 5.12; N, 47.44. Found: C, 19.69; H, 5.08; N, 47.88.

The cobalt(II) complex $[CoL_2(HL)]$ was obtained as dark purple pillar-shaped crystals from a warm aqueous solution (100 mL) containing $[Co^{II}(CH_3COO)_2]\cdot 4H_2O$ (10 mmol) and HL (20 mmol) under nitrogen.[9] Anal. Calcd for $CoC_6H_{16}N_{12}O_6$: Co, 14.33; C, 17.53; H, 3.92; N, 40.88. Found: Co,14.32; C,17.75; H, 3.79; N, 40.80. The nickel(II) complex $[NiL_2(HL)]$ was obtained as brick-red pillar crystals according to the procedure described by Endres et al.[10a] Anal. Calcd for $NiC_6H_{16}N_{12}O_6$: Ni, 14.28; C, 17.54; H, 3.92; N, 40.90. Found: Ni, 14.03; C, 17.90; H, 4.01; N, 40.71. The copper(II) complex $[CuL_2(HL)]$ was obtained as brown needle crystals according to the method described by Endres et al.[11] Anal. Calcd for $CuC_6H_{16}N_{12}O_6$: Cu, 15.28; C, 17.33; H, 3.88; N, 40.42. Found: Cu, 15.11; C, 17.13; H, 3.92; N, 40.55.

**Magnetic Studies.** Magnetic susceptibility data were collected on a Toei Kogyo Model VSM3-15 vibrating-sample magnetometer and a Quantum Design Model MPMS-5S SQUID magnetometer. The magnetic susceptibility was measured on microcrystalline samples of about 70 mg under a field of 1 T in the temperature range 2−300 K. All the observed susceptibilities were corrected for diamagnetism estimated from Pascal's constants.[15] ESR spectra were recorded on a JEOL JES-RE3X spectrometer operating at X-band frequencies with a magnetic field modulation of 100 kHz. Microwave frequency was measured with an Advantest TR5212 microwave counter, and the magnetic field values of signals were measured with a JEOL ES-FC4 NMR Gauss meter.

**Calculation of Molecular Orbitals by the DV-Xα Method.** Molecular orbitals of the complex monomers and dimers $ML_2$ and $2ML_2$ were calculated by the unrestricted DV-Xα method[16] on a Sony model NWS-5000UF net work station. The structures of each monomer and dimer are equivalent to those of a complex molecule and a pair of adjacent complex molecules in the corresponding stack chain determined crystallographically,[9−11] respectively. Thus, because of their $C_i$ symmetry, the coordinate employed for the monomers has its origin at the position of the central metal (M1) and its *XY* plane on the molecular plane containing four nitrogen atoms (N2, N6, N15, and N19), while that for the dimers has its origin at the center of symmetry and its *XY* plane parallel to the planes of the monomer units, one with the atoms M1, N2, N6, N15, and N19 and the other with the atoms M28, N29, N33, N42, and N46, as shown in Figure 1. Basis sets are 1s for H, 1s−2p for C, N, and O, and 1s−4p for Co, Ni, and Cu. Accordingly, the number of types of atoms is 14 for the monomers and 27 for the dimers, while the number of types of orbitals is 37 for the monomers and 66 for the dimers. All the calculations were performed using the exchange parameter α fixed at 0.7, until the difference between the input and output values of each atomic orbital population was less than $1 \times 10^{-5}$ electrons for the monomers and less than $2 \times 10^{-5}$ electrons for the dimers.

## Results

**Magnetic Behaviors.** The magnetic behavior of the cobalt(II) complex $[CoL_2(HL)]$ is shown as $\chi_m T$ against $T$ in Figure 2a, where $\chi_m$ denotes molar magnetic susceptibility and $T$ denotes temperature. From Figure 2a, the $\chi_m T$ value is 0.540 emu K/mol at 298 K, indicating that its effective magnetic moment $\mu_{eff}$ is equal to 2.08 $\mu_B$; $\mu_B$ denotes Bohr magneton. Assuming that the complex is isotropic, the spin quantum

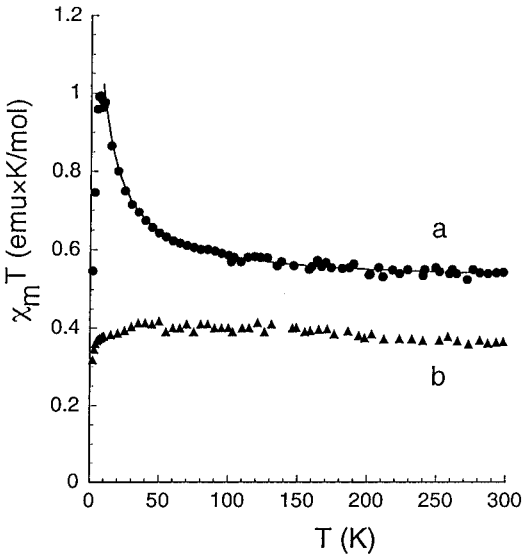


**Figure 2.** Temperature dependence of $\chi_m T$ for (a) [$CoL_2$(HL)] and (b) [$CuL_2$(HL)]. The solid line corresponds to the best fit calculated as described in the text.

number $S$ can be estimated from the equation $\mu_{eff}/\mu_B = g[S(S+1)]^{1/2}$, where $g$ is a $g$-factor. If this isotropic $g$ value is 2.35 as described below, $S$ is equal to 0.52, indicating that the cobalt(II) complex has an $S = {}^1/_2$ ground state, i.e., a low-spin state. In Figure 2a, a marked rise in $\chi_m T$ at temperatures lower than 50 K indicates a transition to a phase with dominant ferromagnetic interactions. On the basis of the crystallographic information on [$CoL_2$(HL)], this result could be reasonably interpreted in terms of a dominant ferromagnetic spin-ordering within the stack chain along the *b*-axis and a secondary antiferromagnetic interaction between the chains in the *ab* plane. Thus, we assume tentatively the isotropic $S = {}^1/_2$ Heizenberg model based on a high-temperature Padé expansion (eq 1),[17] modified by the addition of a mean-field correction (eq 2) to account for the interchain interactions,[18] where $K = J/2kT$; $J$ is the ferromagnetic coupling constant, $Z$ is the number of nearest-neighbor chains ($Z = 2$ in this study), $J'$ is the exchange integral for the magnetic interaction between the nearest-neighbor chains, and the other symbols have their usual meanings.

$$\chi_m' T = (N\mu_B{}^2 g^2/4k)\{1.0 + 5.797\,991\,6K + 16.902\,653K^2 + 29.376\,885K^3 + 29.832\,959K^4 + 14.036\,918K^5)/(1.0 + 2.797\,991\,6K + 7.008\,678\,0K^2 + 8.653\,864\,4K^3 + 4.574\,311\,4K^4)\}^{2/3} \quad (1)$$

$$\chi_m(\text{corr}) = \chi_m'/\{1 - (2ZJ'/Ng^2\mu_B{}^2)\chi_m'\} \quad (2)$$

Looking for the minimum of the factor $R$ defined as $R = \Sigma\{(\chi_m T)^{calc} - (\chi_m T)^{obs}\}^2/\Sigma\{(\chi_m T)^{obs}\}^2$ by the Gauss−Newton method,[19] the parameter values of $J$, $J'$, and $g$ were determined to be consistent with the observed results in Figure 2a as follows: $J = 13.5K$, $J' = -0.005K$, and $g = 2.35$ for $R = 9.36 \times 10^{-3}$ at temperatures 10−298 K. The theoretical curve given by the solid line in Figure 2a is in good agreement with the experimental data. This indicates the existence of ferromagnetic intrachain interactions along the *b*-axis accompanied by a very weak interchain antiferromagnetic interaction in the *ab* plane.

The magnetic data of [$CuL_2$(HL)] are plotted as $\chi_m T$ against $T$ in Figure 2b. Because the value of $\chi_m T$ is equal to 0.37 emu K/mol at room temperature, the $\mu_{eff}$ value is 1.73 $\mu_B$, which is consistent with $S = 0.48$, provided its isotropic $g$ value is equal to 2.064 as obtained by the electron spin resonance (ESR) measurement. In Figure 2b, the $\chi_m T$ value very slightly

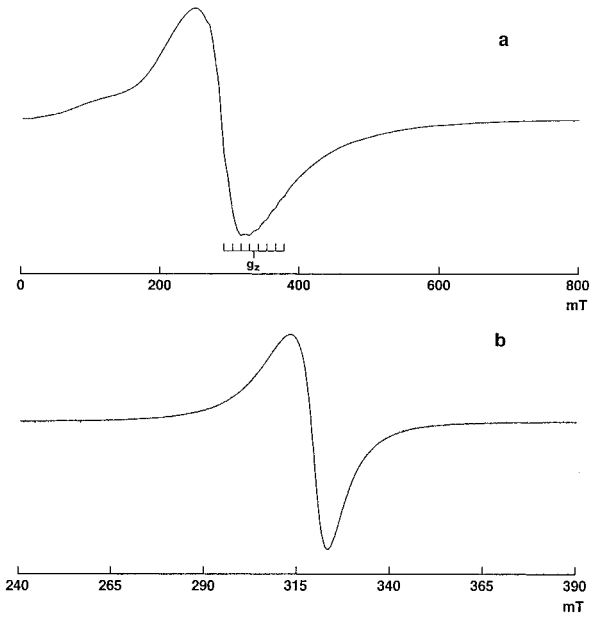


**Figure 3.** ESR spectra of (a) [$CoL_2$(HL)] and (b) [$CuL_2$(HL)] at 173 K.

increases down to ca. 30K, indicating the existence of a very weak ferromagnetic interaction in [$CuL_2$(HL)]. This ferromagnetic interaction is so weak that [$CuL_2$(HL)] is assumed to be paramagnetic in an $S = {}^1/_2$ ground state.

The observed $\chi_m$ values of [$NiL_2$(HL)] were about $-1.49 \times 10^{-4}$ emu/mol not dependent on temperature, which are almost equal to the calculated value based on diamagnetism from Pascal's constants: $-1.39 \times 10^{-4}$ emu/mol.[20] This result means that the complex [$NiL_2$(HL)] is a usual diamagnetic compound.

**ESR Spectra.** ESR spectra of [$CoL_2$(HL)] and [$CuL_2$(HL)] are shown in Figures 3a and 3b, respectively. The ESR spectrum of [$CoL_2$(HL)] is characterized by the combination of a very broad band centered at an average $g$ value ($g_{av}$) of 2.35 with a very weak but distinct hyperfine splitting (hfs) pattern centered at a $g_z$ value of 2.012, which is often observed in $Co^{II}(Hdmg)_2$ ($H_2$dmg = butane-2,3-dione dioxime)[21] and results from the interaction of the unpaired electron with the $^{59}$Co nucleus ($I = {}^7/_2$), with $A_{Co} = 12$ mT. The absence of any hfs signal from $^{14}$N ($I = 1$) nuclei on the apical sites means that the interaction between Co and N atoms is as weak as in the case of $Co^{II}(Hdmg)_2$ in frozen water and alcoholic solvents and much weaker than that observed in strongly coordinating media like pyridine.[21] The very broad absorption would be due to the ferromagnetic spin-ordering within the stack chain described above, because the broadening of ESR spectra by such ordering has often been observed on $Cu^{II}$ and $Mn^{II}$ complexes.[22] The ESR spectra of [$CoL_2$(HL)] down to 123 K are almost the same as that shown in Figure 3a, except for a slight increase in intensity with a decrease in temperature.

On the other hand, the ESR spectrum of [$CuL_2$(HL)] exhibits a slightly anisotropic absorption band centered at a $g_{av}$ value of 2.064, with a width of peak to peak of 10.24 mT, as shown in Figure 3b. The observed values of $g_{av}$ and the peak to peak width are in good agreement with the result reported by Endres et al.[11] The ESR spectra of [$CuL_2$(HL)] down to 123 K are almost the same as that in Figure 3b, except for a gradual increase in intensity with a decrease in temperature. It is noted that the ESR spectrum of [$CuL_2$(HL)] is much sharper than that of [$CoL_2$(HL)] in Figure 3, implying that the complex [$CuL_2$-(HL)] has noncoupled spins. The complex [$NiL_2$(HL)] exhibited only very weak bands, probably due to some impurities.

**MO Calculations by the DV-Xα Method.** The calculated one-electron energy level diagrams for the monomers $ML_2$ (M

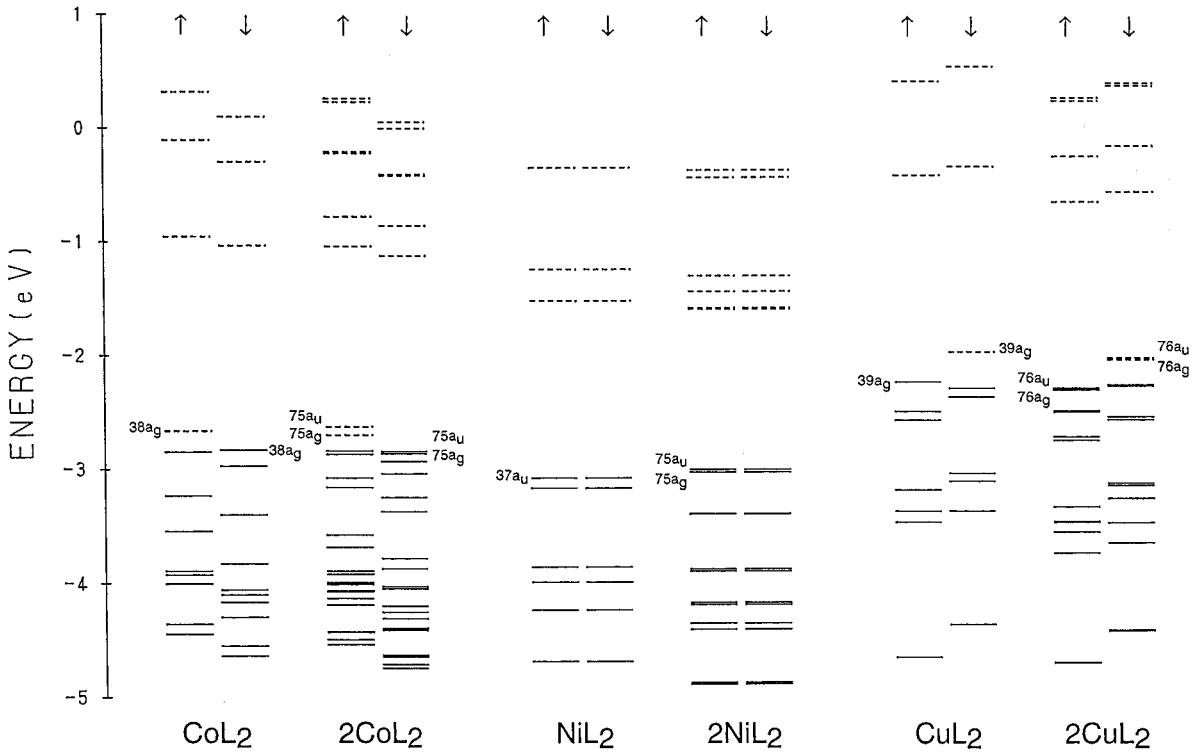


**Figure 4.** Electronic levels of the monomers $ML_2$ and the dimers $2ML_2$ (M = $Co^{II}$, $Ni^{II}$, and $Cu^{II}$). The MOs for up spin (↑) and down spin (↓) are arranged in the left and right columns for each molecule, respectively. Solid and broken lines denote occupied and unoccupied molecular orbitals, respectively. It does not matter whether the POMOs have up spins or down spins.

= $Co^{II}$, $Ni^{II}$, and $Cu^{II}$) are shown in Figure 4, where it does not matter whether the unpaired electron is up spin (↑) or down spin (↓). From Figure 4, the monomers $CoL_2$ and $CuL_2$ are spin-polarized to have an $S = {}^1/_2$ ground state, i.e., a low-spin state; on the other hand, the monomer $NiL_2$ is nonspin-polarized to fall in a singlet ground state. The results from Mulliken's population analysis on these monomers are summarized in Table 1. Every atom on each monomer has the number of electrons consistent with that expected on the basis of electronegativity, considering that the N atoms of amino groups have higher electron densities than those of oxime groups because in the former the nitrogens are directly bound to hydrogen atoms with a lower electronegativity. The $CoL_2$ has the partially occupied molecular orbital (POMO) $38a_g$. The MO $38a_g{\downarrow}$ with an unpaired electron of $CoL_2$ consists of the atomic orbitals of $3d_{zx}$ (on Co), $2p_z$ (on C, N, and O) and $2p_x$ (on N5 and N18), characterized as a $\pi$-type MO developing along the $Z$-axis (Figure 5a). There is little difference between the MO $38a_g{\uparrow}$ for up spin and the MO $38a_g{\downarrow}$ for down spin, because the monomer $CoL_2$ is a low-spin compound. On the other hand, the MO $39a_g{\uparrow}$ with an unpaired electron of $CuL_2$ is an antibonding $\pi$ system developed on the molecular plane $Z = 0$, principally consisting of the $3d_{xy}$ (Cu), the 2s (C8, C21, N2, N6, N15, and N19), the $2p_x$ (N2, N6, N15, N19, and O), and the $2p_y$ bases (C8, C21, N2, N6, N15, N19, and O) with a slight superposition of the $2p_z$ bases (N5, N18, O7, and O20) (Figure 5c). There is also little difference between the MO $39a_g{\uparrow}$ and the MO $39a_g{\downarrow}$ for $CuL_2$. The highest occupied molecular orbital (HOMO) $37a_u$ of $NiL_2$ is a $\pi$-type MO, consisting of mainly $2p_z$ atomic orbitals of the ligands $L_2$ with little contribution from atomic orbitals on the central Ni (Figure 5b).

The differential spin densities ($\Delta\rho{\uparrow\downarrow}$) of $CoL_2$ and $CuL_2$ are shown in Figure 6, where $\Delta\rho{\uparrow\downarrow} = \rho{\uparrow} - \rho{\downarrow}$; $\rho{\uparrow}$ and $\rho{\downarrow}$ are spin densities of up spins and down spins, respectively. The monomer $CoL_2$ has a differential spin density delocalized over the whole molecule and developed along the $Z$-axis; thus it possesses a large $\Delta\rho{\uparrow\downarrow}$ value of $-0.068\ 28e$ even on N5 and N18 at apical sites of Co atoms of the neighboring complex molecules in the stack chain (Table 1). On the other hand, the monomer $CuL_2$, being quite different from $CoL_2$, has a localized differential spin density predominantly on the central Cu atom and the nitrogen (N2, N6, N15, and N19) and oxygen atoms surrounding the Cu atom, with very low differential spin densities on N5 and N18 atoms. Moreover, the differential spin density of $CuL_2$ develops predominantly on its molecular plane $Z = 0$. Accordingly, the difference in $\Delta\rho{\uparrow\downarrow}$ between $CoL_2$ and $CuL_2$ strongly suggests that the magnetic interactions between neighboring molecules in the stack chain are stronger in the complex [$CoL_2$(HL)] than in the complex [$CuL_2$(HL)].

The calculated one-electron energy level diagrams for the complex dimers $2ML_2$ (M = $Co^{II}$, $Ni^{II}$, and $Cu^{II}$) are also shown in Figure 4. From Figure 4, the cobalt(II) and copper(II) dimers are spin-polarized to a triplet ground state, although the nickel-(II) dimer still has a singlet ground state because of its nonspin polarization. The unpaired electrons of $2CoL_2$ exist in the molecular orbitals $75a_g{\downarrow}$ and $75a_u{\downarrow}$. The contour maps of the $75a_g{\downarrow}$ and $75a_u{\downarrow}$ of $2CoL_2$ are shown in Figure 7. It is worth noting that the $75a_g{\downarrow}$ and $75a_u{\downarrow}$ of $2CoL_2$ can be approximately represented by superposition of the $38a_g{\downarrow}$ of the monomer $CoL_2$ on another $38a_g{\downarrow}$ symmetrically and asymmetrically for the $C_i$ symmetry, respectively,[23] from the resemblance of the contour map between the $75a_g{\downarrow}$ or $75a_u{\downarrow}$ of $2CoL_2$ and the $38a_g{\downarrow}$ of $CoL_2$. On the other hand, the unpaired electrons of $2CuL_2$ are in the molecular orbitals $76a_g{\uparrow}$ and $76a_u{\uparrow}$. Comparing their contour maps in Figure 8 with the contour map in Figure 5c, the MOs $76a_g{\uparrow}$ and $76a_u{\uparrow}$ of the dimer $2CuL_2$ are also well represented by superposing the MO $39a_g{\uparrow}$ with an unpaired electron of the monomer $CuL_2$ on another $39a_g{\uparrow}$ symmetrically and asymmetrically with respect to the $C_i$ symmetry, respectively.[24] The contour map of the differential spin density of $2CoL_2$ is shown in Figure 9a. In contrast with the case of the monomer $CoL_2$ (Figure 6a), the differential spin density of $2CoL_2$ increases in the region where the monomer units overlap with each other. On the basis of the results from Mulliken's population analysis

**TABLE 1: Atomic Populations and Differential Atomic Populations of the Monomer $ML_2$ and the Dimer $2ML_2$ (M = $Co^{II}$, $Ni^{II}$, and $Cu^{II}$)**[a,b]

| atom | $CoL_2$ | $2CoL_2$ | $NiL_2$ | $2NiL_2$ | $CuL_2$ | $2CuL_2$ |
|---|---|---|---|---|---|---|
| M(1,28) | 26.712 46 | 26.711 20 | 27.590 26 | 27.590 42 | 28.490 99 | 28.586 34 |
| | −0.305 00 | −0.342 56 | 0 | 0 | +0.173 07 | +0.187 00 |
| N(2,42) | 7.131 79 | 7.156 19 | 7.143 76 | 7.194 88 | 7.247 73 | 7.270 60 |
| | −0.038 49 | −0.014 81 | 0 | 0 | +0.088 11 | +0.082 56 |
| N(15,29) | | 7.104 94 | | 7.156 40 | | 7.211 65 |
| | | −0.072 98 | | 0 | | +0.088 13 |
| C(4,44) | 5.967 56 | 6.024 70 | 5.949 48 | 5.954 52 | 6.024 89 | 6.042 45 |
| | −0.040 06 | −0.018 62 | 0 | 0 | −0.004 77 | −0.00397 |
| C(17,31) | | 5.970 76 | | 5.946 26 | | 6.024 14 |
| | | −0.021 04 | | 0 | | −0.006 72 |
| O(3,43) | 8.406 58 | 8.440 47 | 8.388 70 | 8.396 32 | 8.410 01 | 8.436 64 |
| | −0.100 26 | −0.045 21 | 0 | 0 | +0.027 11 | +0.025 88 |
| O(16,30) | | 8.372 99 | | 8.362 40 | | 8.404 32 |
| | | −0.181 59 | | 0 | | +0.027 16 |
| N(5,45) | 7.530 12 | 7.519 54 | 7.505 02 | 7.538 76 | 7.898 19 | 7.918 33 |
| | −0.068 28 | −0.033 76 | 0 | 0 | −0.001 55 | −0.000 95 |
| N(18,32) | | 7.468 20 | | 7.537 12 | | 7.851 97 |
| | | −0.104 50 | | 0 | | −0.000 83 |
| N(6,46) | 7.116 03 | 7.125 77 | 7.108 68 | 7.099 64 | 7.176 04 | 7.166 47 |
| | −0.053 09 | −0.018 71 | 0 | 0 | +0.112 06 | +0.103 23 |
| N(19,33) | | 7.104 37 | | 7.117 52 | | 7.180 94 |
| | | −0.065 33 | | 0 | | +0.121 36 |
| C(8,48) | 5.988 12 | 6.031 02 | 5.968 62 | 5.989 94 | 6.010 96 | 6.045 11 |
| | −0.005 28 | +0.000 58 | 0 | 0 | −0.015 14 | −0.013 25 |
| C(21,35) | | 5.971 10 | | 5.945 76 | | 5.973 49 |
| | | −0.006 46 | | 0 | | −0.014 77 |
| O(7,47) | 8.360 59 | 8.370 41 | 8.422 72 | 8.417 16 | 8.464 31 | 8.468 41 |
| | −0.041 33 | −0.009 19 | 0 | 0 | +0.218 05 | +0.179 83 |
| O(20,34) | | 8.351 21 | | 8.409 54 | | 8.449 92 |
| | | −0.057 79 | | 0 | | +0.245 92 |
| N(9,49) | 7.573 11 | 7.607 82 | 7.400 54 | 7.396 70 | 7.522 51 | 7.563 53 |
| | −0.017 85 | −0.004 78 | 0 | 0 | −0.014 41 | −0.008 25 |
| N(22,36) | | 7.588 60 | | 7.392 56 | | 7.511 16 |
| | | −0.020 50 | | 0 | | −0.010 98 |
| H(10,50) | 0.670 77 | 0.689 31 | 0.672 98 | 0.653 90 | 0.612 74 | 0.603 23 |
| | +0.003 09 | +0.003 41 | 0 | 0 | −0.001 72 | −0.001 65 |
| H(23,37) | | 0.673 25 | | 0.668 62 | | 0.599 93 |
| | | +0.002 45 | | 0 | | −0.001 67 |
| H(11,51) | 0.848 62 | 0.830 36 | 0.796 02 | 0.800 44 | 0.200 00 | 0.190 78 |
| | +0.000 88 | +0.001 70 | 0 | 0 | −0.000 06 | −0.000 04 |
| H(24,38) | | 0.815 78 | | 0.785 82 | | 0.165 46 |
| | | +0.005 60 | | 0 | | −0.000 10 |
| H(12,52) | 0.393 94 | 0.394 51 | 0.399 94 | 0.357 06 | 0.422 58 | 0.400 17 |
| | +0.012 02 | +0.000 57 | 0 | 0 | +0.000 02 | +0.000 03 |
| H(25,39) | | 0.397 53 | | 0.342 94 | | 0.421 89 |
| | | +0.001 93 | | 0 | | +0.000 03 |
| H(13,53) | 0.321 05 | 0.320 29 | 0.804 70 | 0.807 40 | 0.743 23 | 0.710 80 |
| | +0.000 45 | +0.000 15 | 0 | 0 | +0.000 67 | +0.000 58 |
| H(26,40) | | 0.326 88 | | 0.778 58 | | 0.765 62 |
| | | +0.000 50 | | 0 | | +0.000 76 |
| H(14,54) | 0.835 48 | 0.833 04 | 0.643 72 | 0.667 28 | 0.521 30 | 0.516 99 |
| | +0.000 74 | +0.000 24 | 0 | 0 | +0.005 08 | +0.000 33 |
| H(27,41) | | 0.799 72 | | 0.692 10 | | 0.519 65 |
| | | +0.000 68 | | 0 | | +0.000 39 |

[a] Differential atomic populstion is defined as $N_x\uparrow - N_x\downarrow$, where $N_x\uparrow$ and $N_x\downarrow$ are atomic populations for up spin (↑) and down spin (↓) on an atom X, respectively. [b] Atomic population and differential atomic population are given on the upper and the lower line for each atom, respectively. The values for the equivalent atoms in the monomers are omitted for simplicity.

in Table 1, the differential spin density increases in the cobalts Co1 and Co28, in the nitrogens N18 and N32 occupying apical sites of the cobalts, and in the nitrogens N15 and N29 coordinating to the cobalts on the planes of the monomer units, generating two pathways to couple the cobalt atoms Co1 and Co28 together (one is Co1−N32−C31−N29−Co28, and the other is Co28−N18−C17−N15−Co1). Further, although the differential spin density of $2CoL_2$ decreases relatively in the portion where the two monomer units do not overlap with each other, the large $\Delta\rho\uparrow\downarrow$ value (−0.033 76*e*) is still maintained on N5 and N45, which are free in the dimer model, but occupy apical sites of the neighboring complex molecules in the stack chain. In contrast, the differential spin density of the copper(II) dimer $2CuL_2$ is principally characterized by the localization of differential spins near each copper atom and the atoms surrounding the copper in Figure 9b. This is very similar to the character of the monomer $CuL_2$ described earlier (Figure 6b). It is worth noting the very low density of differential spins on N18 and N32 (−0.000 83*e* in Table 1) occupying apical sites of the coppers and on N5 and N45 (−0.000 95*e* in Table 1) at apical sites of the neighboring complex molecules in the stack chain of the real system. Thus, this characteristic of the differential spin density for $2CuL_2$ clearly suggests that two monomer units are rather isolated from each other owing to the lack of pathways for superexchange between the metals, which exist in the case of $2CoL_2$.

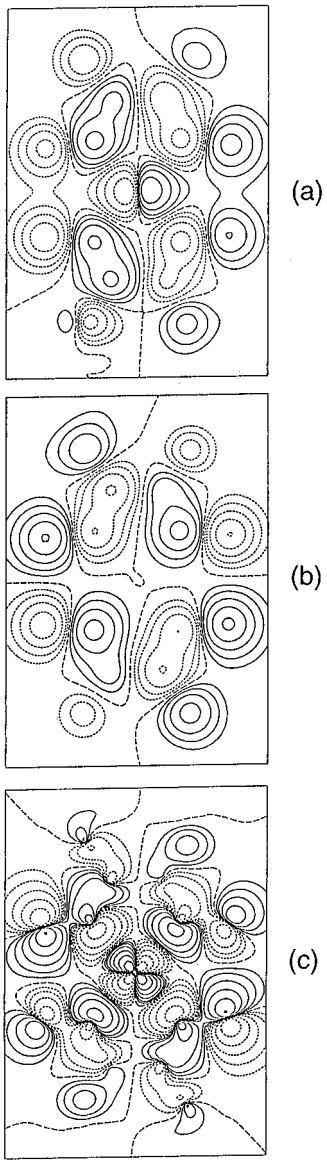


**Figure 5.** Contour maps of molecular orbitals of the monomers $ML_2$: (a) the POMO $38a_g{\downarrow}$ of $CoL_2$ on the plane $Z = 1.0$ au, (b) the HOMO 37 $a_u{\uparrow}({\downarrow})$ of $NiL_2$ on the plane $Z = 1.0$ au, and (c) the POMO $39ag{\uparrow}$ of $CuL_2$ on the plane $Z = 0$ au. Solid, dotted, and broken lines denote positive, negative, and zero, respectively.

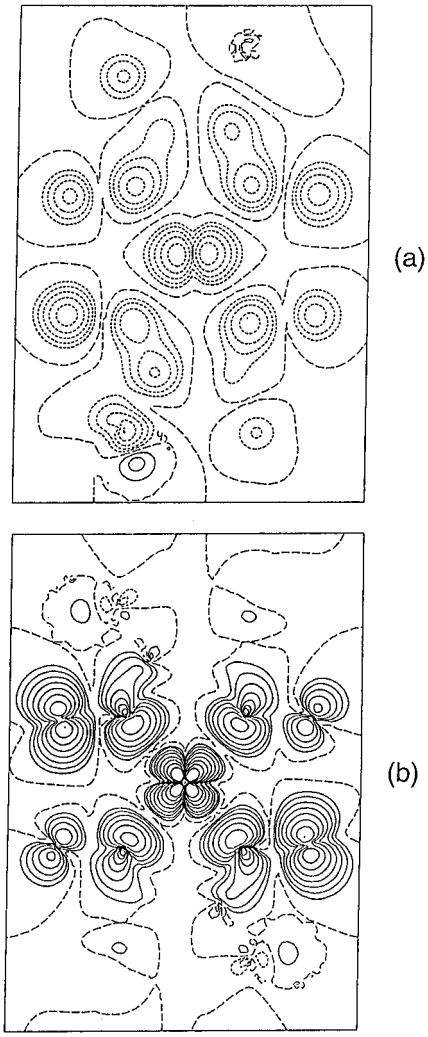


**Figure 6.** Contour maps of the differential spin density $\Delta\rho{\uparrow\downarrow}$ of (a) $CoL_2$ on the plane $Z = 1.0$ au and (b) $CuL_2$ on the plane $Z = 0$ au. Solid, dotted, and broken lines denote positive, negative, and zero, respectively.

## Discussion

We have revealed that the divalent metal complexes with diaminoglyoxime [$ML_2$(HL)] (M = $Co^{II}$, $Ni^{II}$, and $Cu^{II}$), in spite of their resemblance in stacking mode, show quite different magnetic behaviors: the $Co^{II}$ complex exhibits ferromagnetic interactions along the stacking chain, while the $Ni^{II}$ complex is diamagnetic, and the $Cu^{II}$ complex is almost paramagnetic. In order to understand the nature of the magnetism of these diaminoglyoxime complexes, we investigate the magnetic interactions between monomer units in the dimer model $2ML_2$. The magnetic properties of a binuclear complex a−b, where a (or b) denotes a monomeric fragment with $S_a = {}^1/_2$ (or $S_b = {}^1/_2$), have been qualitatively examined on the basis of the MOs $\phi_a$ and $\phi_b$ of unpaired electrons for the fragments a and b, respectively.[1b,25] Kahn et al. reported that the singlet−triplet splitting of such a system results from competition between two antagonist terms; one ($J_F$), a ferromagnetic contribution, is proportional to the two-electron exchange integral between $\phi_a$ and $\phi_b$, and the other ($J_{AF}$), an antiferromagnetic contribution, is proportional to the square of the overlap integral of the MOs.[1b] The $J_F$ term depends mainly on the zones of strong overlap density $\phi_a\phi_b$, irrespective of their sign. The $J_{AF}$ term, on the other hand, depends on the balance between a positive and a negative zone of the overlap density. According to this concept, we can roughly predict that the dimer $2CoL_2$ is more ferromagnetic than the dimer $2CuL_2$ and that the $2CuL_2$ is almost paramagnetic because $J_F(2CuL_2) \ll J_F(2CoL_2)$ and $J_{AF}(CuL_2) \approx J_{AF}(2CoL_2) \approx 0$, provided that the MOs $\phi_a$ and $\phi_b$ are the MO $38a_g{\downarrow}$ for $CoL_2$ and the MO $39a_g{\uparrow}$ for $CuL_2$. In this study, we undertake to evaluate directly the magnetic interactions between the monomer units in the dimer $2ML_2$, on the basis of the molecular orbital calculations of the monomer $ML_2$ and the dimer $2ML_2$, using the unrestricted DV-Xα method.

Generally, magnetism results from the exchange interactions of electrons. According to the Xα method, the spin splitting of the $k$th molecular orbital $\phi_{A,k}$ of a molecule A, $\Delta\epsilon_{A,k}{\uparrow\downarrow}^\circ$, is approximately expressed as a difference of exchange interaction between the up spin and the down spin, as in eq 3.[26]

$$\Delta\epsilon_{A,k}{\uparrow\downarrow}^\circ \approx -3\alpha(3/4\pi)^{1/3}\{\langle\phi_{A,k}{\uparrow}|\rho_A{\uparrow}^{1/3}|\phi_{A,k}{\uparrow}\rangle - \langle\phi_{A,k}{\downarrow}|\rho_A{\downarrow}^{1/3}|\phi_{A,k}{\downarrow}\rangle\} \quad (3)$$

As a minute variation of the exchange interaction can be described as a deviation of the spin splitting under a small perturbation, as shown in Appendix A, we can safely estimate the exchange interaction in a molecular system from the spin splitting. Thus, we have concentrated our discussion on the

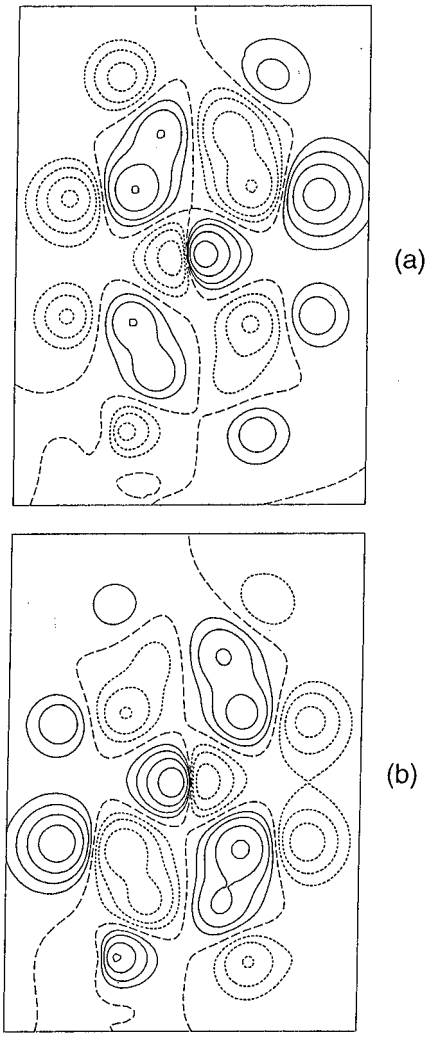


**Figure 7.** Contour maps of the POMOs (a) $75a_g\downarrow$ and (b) $75a_u\downarrow$ of the dimer $2CoL_2$ on the plane, the Z value of which is by +1.0 au larger than that of the plane of the monomer unit with $Z < 0$. Solid, dotted, and broken lines are the same as in Figure 5.

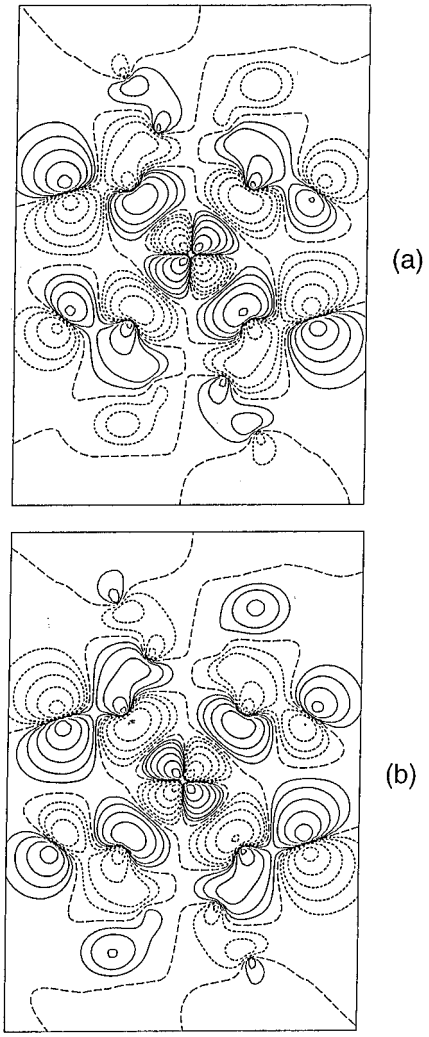


**Figure 8.** Contour maps of the POMOs (a) $76a_g\uparrow$ and (b) $76a_u\uparrow$ of the dimer $2CuL_2$ on the plane of the molecular unit with $Z < 0$. Solid, dotted, and broken lines are the same as in Figure 5.

spin splitting of the POMOs of the dimer $2ML_2$ in order to examine the magnetism of $2ML_2$.

We consider a dimer A−B belonging to $C_i$ symmetry with paramagnetic monomer units A ($S_A = 1/2$) and B ($S_B = 1/2$) weakly interacting with each other as the model for $2ML_2$ (M = $Co^{II}$ and $Cu^{II}$). Assuming that the POMOs of the dimer, $\phi_{A-B,\zeta}$, are expressed by superposition of the POMOs of the monomers A and B, $\phi_{A,l}$ and $\phi_{B,l}$, and that the spin density of the dimer, $\rho_{A-B}\uparrow$ (or $\rho_{A-B}\downarrow$), is also described by superposition of the spin densities of the monomers A and B, $\rho_A\uparrow$ (or $\rho_A\downarrow$) and $\rho_B\uparrow$(or $\rho_B\downarrow$), eqs 4 and 5 hold for the up spin.

$$\phi_{A-B,\zeta}\uparrow \approx \phi_{A,l}\uparrow + \phi_{B,l}\uparrow \quad (4)$$

$$\rho_{A-B}\uparrow \approx \rho_A\uparrow + \rho_B\uparrow \quad (5)$$

The symmetry of the dimer A−B requires the following relations for the up spin,

$$\phi_{A,l}\uparrow = \pm R(\phi_{B,l}\uparrow) \quad (6)$$

$$\rho_A\uparrow = \pm R(\rho_B\uparrow) \quad (7)$$

where R denotes the symmetry operation for the center of symmetry. Similar relations hold for the down spin. The cobalt(II) and the copper(II) dimer $2ML_2$ (M=Co, and Cu) satisfies eqs 4−7, as described in the preceding section. According to Appendix B, the magnetic interaction between the monomer units in the dimer A−B, $J_{A-B}$, can be estimated from the difference of the spin splitting of the POMO between the monomer and the dimer, as expressed by eq 8,

$$J_{A-B} = (\Delta\epsilon_{A-B,\zeta(+)}{}^{\uparrow\downarrow} - \Delta\epsilon_{A,k}{}^{\uparrow\downarrow\circ}) + (\Delta\epsilon_{A-B,\zeta(-)}{}^{\uparrow\downarrow} - \Delta\epsilon_{A,k}{}^{\uparrow\downarrow\circ}) \quad (8)$$

where + and − indicate the symmetry and the asymmetry for the operation R, respectively. This relationship clearly shows that the dimer A−B is ferromagnetic if $J_{A-B} > 0$, paramagnetic if $J_{A-B} = 0$, and antiferromagnetic if $J_{A-B} < 0$.

For the cobalt(II) dimer $2CoL_2$ which has the POMOs $75a_g$ and $75a_u$, the magnetic interaction $J_{2Co}$ is expressed by the following equation from eq 8,

$$J_{2Co} = (\Delta\epsilon_{2Co,75au}{}^{\uparrow\downarrow} - \Delta\epsilon_{Co,38ag}{}^{\uparrow\downarrow\circ}) + (\Delta\epsilon_{2Co,75ag}{}^{\uparrow\downarrow} - \Delta\epsilon_{Co,38ag}{}^{\uparrow\downarrow\circ}) \quad (9)$$

and similarly the magnetic interaction for $2CuL_2$ is expressed by eq 10.

$$J_{2Cu} = (\Delta\epsilon_{2Cu,76au}{}^{\uparrow\downarrow} - \Delta\epsilon_{Cu,39ag}{}^{\uparrow\downarrow\circ}) + (\Delta\epsilon_{2Cu,76ag}{}^{\uparrow\downarrow} - \Delta\epsilon_{Cu,39ag}{}^{\uparrow\downarrow\circ}) \quad (10)$$

The results calculated from eqs 9 and 10 are collected in Table 2. These results show that $2CoL_2$ has a much larger $J$ value than $2CuL_2$. However, it must be mentioned that the calculated

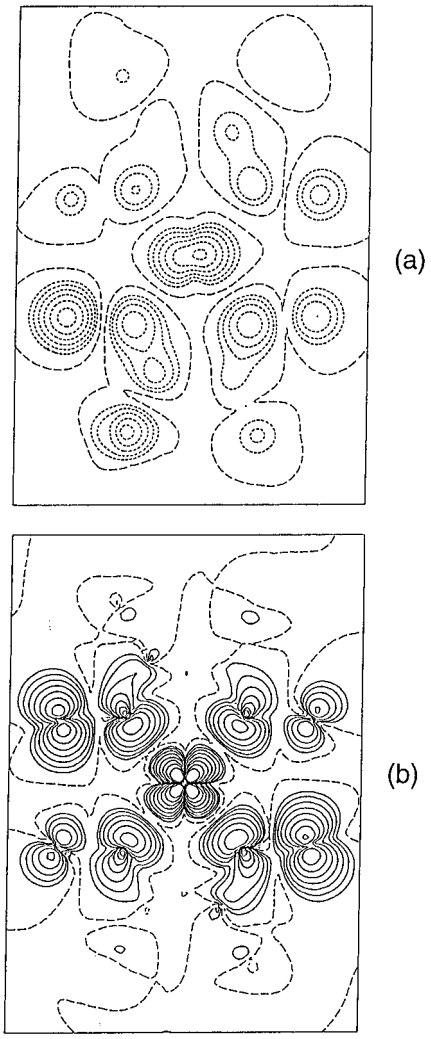


**Figure 9.** Contour maps of the differential spin density $\Delta\rho\uparrow\downarrow$ of (a) $2CoL_2$ on the plane, the $Z$ value of which is by $+1.0$ au larger than that of the plane of the monomer unit with $Z < 0$ and of (b) $2CuL_2$ on the plane of the monomer unit with $Z < 0$. Solid, dotted, and broken lines are the same as in Figure 6.

**TABLE 2: Magnetic Interactions between Monomer Units in the Dimer 2ML2 (M = $Co^{II}$ and $Cu^{II}$)**

| dimer | J(eV)[a] |
|---|---|
| $2CoL_2$ | 0.051 25 |
| $2CuL_2$ | 0.002 84 |

[a] These values were obtained from eqs 9 and 10.

*J* values are much larger than those expected from the experiments (the observed value of the ferromagnetic intrachain interactions for $[CoL_2(HL)]$ is 13.5K, i.e., 0.001 16 eV). This is probably due to a larger variation of spin density in the dimer model than in the real system. It should be mentioned that $2CoL_2$ has a higher differential spin density in the portion where the monomeric units overlap with each other. In the real stack chain, however, the differential spin density on N5 (or N32) in Figure 1 has to be the same as that on N18 (or N45), because of their equivalence in structure. Thus, considering that the spin splitting depends largely on the differential spin density as described above, the *J* value for the dimer could be larger than that expected in the real system. Taking this into account, it could be concluded that the *J* values for the dimers in Table 2 are satisfactorily consistent with the experimental findings that $[CoL_2(HL)]$ is a linear ferromagnet and $[CuL_2(HL)]$ is paramagnetic.

The $CoL_2$ has the POMO $38a_g\downarrow$ developing along the direction perpendicular to the molecular plane because of the $\pi$ character consisting of the $3d_{zx}$ (Co) and $2p_z$ bases (C, N, and O on the ligands). The $2CoL_2$ has the POMOs $75a_g\downarrow$ and $75a_u\downarrow$, which are expressed by superposition of the POMO $38a_g\downarrow$ of the monomer units on another $38a_g\downarrow$ symmetrically and asymmetrically, respectively, implying larger magnetic interactions between the monomeric units. In comparison with the monomer, the dimer exhibits a marked increase of the differential spin density in the overlapping zone of the monomeric units, as clearly shown in Figure 9a (see the values on N18 (N32), C21 (C35), N15 (N29), O16 (O30), and Co1 (Co28) in Table 1). In particular, the differential spin density on N18 (or N32), which occupies an apical site of Co in each monomeric unit, is more than 1.5 times larger than that on the relevant N in the monomer. Accordingly, this strongly suggests that unpaired spins in the dimer $2CoL_2$ are coupled parallel to each other through the strong exchange interaction between the $3d_{zx}$ orbitals of Co1 (and Co28) and the $2p_z$ orbitals of N32 (and N18) at an apical site of each Co atom. Probably a similar mechanism causes the linear ferromagnetism along the stack chain of the cobalt complex $[CoL_2(HL)]$. Conversely, the copper(II) monomer $CuL_2$ has the POMO $39a_g\uparrow$ developing on the molecular plane owing to a $\pi$ character with the $d_{xy}$ (Cu), and the $2p_x$ and $2p_y$ bases (C, N, and O on the ligands) (Figure 5c). Furthermore, the differential spin density of $CuL_2$ localizes intensively on the central Cu and on the atoms surrounding the metal, N2 (N15), N6 (N19), O3 (O16), and O7 (O20), not on N5 (N18) as coordination sites toward the neighboring complexes in the real stack chain. The dimer $2CuL_2$ has the POMOs $76a_g\uparrow$ and $76a_u\uparrow$, which are characterized by the superposition of the POMO $39a_g\uparrow$ of the monomer on another $39a_g\uparrow$ symmetrically and asymmetrically, respectively, as described before. Thus, in comparison with the dimer $2CoL_2$, the magnetic interaction between the monomeric units in $2CuL_2$ is probably very small because of the orbital mode of the $39a_g\uparrow$ developing on the molecular plane. This prediction is also supported by the differential spin density of $2CuL_2$ in Figure 9b. The differential spin density is extremely low on N18 and N32 ($-0.000$ 83e in Table 1) occupying apical sites of Co28 and Co1, respectively and it fails to channel the superexchange between the Cu metals. Figure 9b well illustrates that the spins in $2CuL_2$ are isolated from each other, declaring that the dimer is virtually paramagnetic. A similar situation may occur in the real stack chain in the crystalline phase of $[CuL_2(HL)]$.

The magnetism of the nickel system $[NiL_2(HL)]$ can be predicted from the calculated results of the monomer $NiL_2$. The monomer $NiL_2$ has only nondegenerated molecular orbitals because of its symmetry $C_i$. Such a molecular system with an even number of electrons usually favors nonspin polarization.

We can conclude from these results that the magnetic behaviors of the divalent metal complexes with diaminoglyoxime $[ML_2(HL)]$ (M=$Co^{II}$, $Ni^{II}$, and $Cu^{II}$) with a slipped-stack mode are precisely predicted from a comparison of the spin splitting of the POMO of the monomer complex $ML_2$ and the dimer complex $2ML_2$ which are equivalent in structure to the relevant moieties in the real stack chain. In addition, the differential spin density of the dimer $2ML_2$ can satisfactorily predict the mechanism of superexchange in the stack chain. Therefore, the method developed in this study will play an important role in the design of novel organomagnetic materials with a variety of stack modes.

**Acknowledgment.** We are grateful to Prof. H. Adachi (Kyoto University) for his kind instruction in the concept of the DV-X$\alpha$ method. We thank Dr. N. Higuchi (Electrotechnical Laboratory) for the measurement of magnetic susceptibility by the SQUID.

## Appendix A

According to the Xα method, the spin splitting of the *k*th molecular orbital $\phi_{A,k}$ for a molecule A, $\Delta\epsilon_{A,k}{}^{\uparrow\downarrow\circ}$, is approximately expressed in the following equation.[26]

$$\Delta\epsilon_{A,k}{}^{\uparrow\downarrow\circ} \approx -3\alpha(3/4\pi)^{1/3}\{\langle\phi_{A,k}{}^{\uparrow}|\rho_A{}^{\uparrow 1/3}|\phi_{A,k}{}^{\uparrow}\rangle - \langle\phi_{A,k}{}^{\downarrow}|\rho_A{}^{\downarrow 1/3}|\phi_{A,k}{}^{\downarrow}\rangle\} \quad \text{(A1)}$$

Let us derive the formula of spin splitting $\Delta\epsilon_{A,k}{}^{\uparrow\downarrow}$, when the molecular orbital and spin density vary minutely under a small perturbation as follows,

$$\phi_{A,k} \rightarrow \phi_{A,k} + \delta\phi_{A,k}$$
$$\rho_A \rightarrow \rho_A + \delta\rho_A$$

From eq A1,

$$\Delta\epsilon_{A,k}{}^{\uparrow\downarrow} \approx -3\alpha(3/4\pi)^{1/3}\{\langle\phi_{A,k}{}^{\uparrow} + \delta\phi_{A,k}{}^{\uparrow}|(\rho_A{}^{\uparrow} + \delta\rho_A{}^{\uparrow})^{1/3}|\phi_{A,k}{}^{\uparrow} + \delta\phi_{A,k}{}^{\uparrow}\rangle - \langle\phi_{A,k}{}^{\downarrow} + \delta\phi_{A,k}{}^{\downarrow}|(\rho_A{}^{\downarrow} + \delta\rho_A{}^{\downarrow})^{1/3}|\phi_{A,k}{}^{\downarrow} + \delta\phi_{A,k}{}^{\downarrow}\rangle\} \quad \text{(A2)}$$

Expanding the the term $(\rho_A + \delta\rho_A)^{1/3}$,

$$\begin{aligned}(\rho_A + \delta\rho_A)^{1/3} &= \{\rho_A(1 + \delta\rho_A/\rho_A)\}^{1/3} \\ &= \rho_A{}^{1/3} + (^1/_3)\delta\rho_A/\rho_A{}^{2/3} + ... \\ &= \rho_A{}^{1/3} + \delta(\rho_A{}^{1/3}) + ... \end{aligned} \quad \text{(A3)}$$

By use of eq A3, eq A2 is rewritten as eq A4.

$$\begin{aligned}\Delta\epsilon_{A,k}{}^{\uparrow\downarrow} &\approx \Delta\epsilon_{A,k}{}^{\uparrow\downarrow\circ} -3\alpha(3/4\pi)^{1/3}[2\{\langle\delta\phi_{A,k}{}^{\uparrow} \mid \rho_A{}^{\uparrow 1/3}|\phi_{A,k}{}^{\uparrow}\rangle - \langle\delta\phi_{A,k}{}^{\downarrow} \mid \rho_A{}^{\downarrow 1/3}|\phi_{A,k}{}^{\downarrow}\rangle\} + \{\langle\phi_{A,k}{}^{\uparrow} \mid \delta(\rho_A{}^{\uparrow 1/3})\,|\phi_{A,k}{}^{\uparrow}\rangle - \langle\phi_{A,k}{}^{\downarrow} \mid \delta(\rho_A{}^{\downarrow 1/3})|\phi_{A,k}{}^{\downarrow}\rangle\}] + ... \\ &\approx \Delta\epsilon_{A,k}{}^{\uparrow\downarrow\circ} -3\alpha(3/4\pi)^{1/3} \delta\{\langle\phi_{A,k}{}^{\uparrow} \mid \rho_A{}^{\uparrow 1/3}|\phi_{A,k}{}^{\uparrow}\rangle - \langle\phi_{A,k}{}^{\downarrow} \mid \rho_A{}^{\downarrow 1/3}|\phi_{A,k}{}^{\downarrow}\rangle\} + ... \end{aligned} \quad \text{(A4)}$$

Thus,

$$\Delta\epsilon_{A,k}{}^{\uparrow\downarrow} - \Delta\epsilon_{A,k}{}^{\uparrow\downarrow\circ} \approx -3\alpha(3/4\pi)^{1/3}\,\delta\{\langle\phi_{A,k}{}^{\uparrow} \mid \rho_A{}^{\uparrow 1/3}|\phi_{A,k}{}^{\uparrow}\rangle - \langle\phi_{A,k}{}^{\downarrow} \mid \rho_A{}^{\downarrow 1/3}|\phi_{A,k}{}^{\downarrow}\rangle\} + ... \quad \text{(A5)}$$

It is shown from eq A5 that the variation of the spin splitting is equal to that of the exchange interaction under a small perturbation.

## Appendix B

We consider a hypothetical dimer A−B belonging to $C_i$ symmetry and consisting of monomer units A and B without any interaction between the monomer units. For this system, the POMOs, $\phi_{A-B,\zeta}{}^{\circ}$, and the spin density $\rho_{A-B}{}^{\circ\uparrow}$ ($\rho_{A-B}{}^{\circ\downarrow}$) are written as eqs A6 and A7 for the up-spin,

$$\phi_{A-B,\zeta}{}^{\circ\uparrow} = (^1/_2)^{1/2}\,(\phi_{A,l}{}^{\uparrow} + \phi_{B,l}{}^{\uparrow}) \quad \text{(A6)}$$
$$\rho_{A-B}{}^{\circ\uparrow} = \rho_A{}^{\uparrow} + \rho_B{}^{\uparrow} \quad \text{(A7)}$$

where $\phi_{A,l}{}^{\uparrow}$ and $\phi_{B,l}{}^{\uparrow}$ are the POMOs for the up spin of the monomer units A and B, respectively. Similar formulas are written for the down spin. The symmetry of the dimer requires the following relations with respect to the symmetry operation for the center of symmetry R,

$$\phi_{B,l}{}^{\uparrow} = \pm R(\phi_{A,l}{}^{\uparrow}), \qquad \phi_{B,l}{}^{\downarrow} = \pm R(\phi_{A,l}{}^{\downarrow}) \quad \text{(A8)}$$
$$\rho_A{}^{\uparrow} = \pm R(\rho_B{}^{\uparrow}), \qquad \rho_A{}^{\downarrow} = \pm R(\rho_B{}^{\downarrow}) \quad \text{(A9)}$$

Also the following relations hold,

$$\langle\phi_{A,m}{}^{\uparrow}|\phi_{B,n}{}^{\uparrow}\rangle = 0, \qquad \langle\phi_{A,m}{}^{\downarrow}|\phi_{B,n}{}^{\downarrow}\rangle = 0 \quad \text{(A10)}$$

where $\phi_{A,m}{}^{\uparrow}$ ($\phi_{A,m}{}^{\downarrow}$) and $\phi_{B,n}{}^{\uparrow}$ ($\phi_{B,n}{}^{\downarrow}$) are the molecular orbitals of the monomers A and B, respectively. The spin splitting of the POMO $\phi_{A-B,\zeta}{}^{\circ}$, $\Delta\epsilon_{A-B,\zeta}{}^{\uparrow\downarrow\circ}$, is written as eq A11 on the basis of eq A1.

$$\Delta\epsilon_{A-B,\zeta}{}^{\uparrow\downarrow\circ} \approx -3\alpha(3/4\pi)^{1/3}\{\langle\phi_{A-B,\zeta}{}^{\circ\uparrow} \mid \rho_{A-B}{}^{\uparrow\circ 1/3}|\phi_{A-B,\zeta}{}^{\circ\uparrow}\rangle - \langle\phi_{A-B,\zeta}{}^{\circ\downarrow}|\rho_{A-B}{}^{\downarrow\circ 1/3}|\phi_{A-B,\zeta}{}^{\circ\downarrow}\rangle\} \quad \text{(A11)}$$

Substituting eqs A6 and A7 into eq A11 and using eqs A8-A10, eq A11 is rewritten as eq A12.

$$\Delta\epsilon_{A-B,\zeta}{}^{\uparrow\downarrow\circ} \approx -3\alpha(3/4\pi)^{1/3}\{\langle\phi_{A,l}{}^{\uparrow}|\rho_A{}^{\uparrow 1/3}|\phi_{A,l}{}^{\uparrow}\rangle - \langle\phi_{A,l}{}^{\downarrow}|\rho_A{}^{\downarrow 1/3}|\phi_{A,l}{}^{\downarrow}\rangle\} \approx \Delta\epsilon_{A,l}{}^{\uparrow\downarrow\circ} \quad \text{(A12)}$$

Thus the spin splitting of the POMO in the hypothetical dimer is approximately equal to that of the relevant monomer itself.

Next, let us consider the dimer system with small interactions between the monomer units. We assume that the POMO $\phi_{A-B,\zeta}$ and spin density $\rho_{A-B}{}^{\uparrow}$ ($\rho_{A-B}{}^{\downarrow}$) are expressed by eqs A13 and A14 for the up spin, respectively.

$$\phi_{A-B,\zeta}{}^{\uparrow} = \phi_{A-B,\zeta}{}^{\circ\uparrow} + \delta\phi_{A-B,\zeta}{}^{\circ\uparrow} \quad \text{(A13)}$$
$$\rho_{A-B}{}^{\uparrow} = \rho_{A-B}{}^{\circ\uparrow} + \delta\rho_{A-B}{}^{\circ\uparrow} \quad \text{(A14)}$$

Similar formulas are written for the down spin. The spin splitting of the POMO $\phi_{A-B,\zeta}$ , $\Delta\epsilon_{A-B,\zeta}{}^{\uparrow\downarrow}$, is represented as eq A15, by use of eqs A4 and A12.

$$\begin{aligned}\Delta\epsilon_{A-B,\zeta}{}^{\uparrow\downarrow} &\approx \Delta\epsilon_{A-B,\zeta}{}^{\uparrow\downarrow\circ} -3\alpha(3/4\pi)^{1/3}\,\delta\{\langle\phi_{A-B,\zeta}{}^{\circ\uparrow}|\rho_{A-B}{}^{\uparrow\circ 1/3}|\phi_{A-B,\zeta}{}^{\circ\uparrow}\rangle - \langle\phi_{A-B,\zeta}{}^{\circ\downarrow}|\rho_{A-B}{}^{\downarrow\circ 1/3}|\phi_{A-B,\zeta}{}^{\circ\downarrow}\rangle\} \\ &\approx \Delta\epsilon_{A,l}{}^{\uparrow\downarrow\circ} -3\alpha(3/4\pi)^{1/3} \times \delta\{\langle\phi_{A-B,\zeta}{}^{\circ\uparrow}|\rho_{A-B}{}^{\uparrow\circ 1/3}|\phi_{A-B,\zeta}{}^{\circ\uparrow}\rangle - \langle\phi_{A-B,\zeta}{}^{\circ\downarrow}|\rho_{A-B}{}^{\downarrow\circ 1/3}|\phi_{A-B,\zeta}{}^{\circ\downarrow}\rangle\} \end{aligned} \quad \text{(A15)}$$

Thus,

$$\Delta\epsilon_{A-B,\zeta}{}^{\uparrow\downarrow} - \Delta\epsilon_{A,l}{}^{\uparrow\downarrow\circ} \approx -3\alpha(3/4\pi)^{1/3}\,\delta\{\langle\phi_{A-B,\zeta}{}^{\circ\uparrow}|\rho_{A-B}{}^{\uparrow\circ 1/3}|\phi_{A-B,\zeta}{}^{\circ\uparrow}\rangle - \langle\phi_{A-B,\zeta}{}^{\circ\downarrow}|\rho_{A-B}{}^{\downarrow\circ 1/3}|\phi_{A-B,\zeta}{}^{\circ\downarrow}\rangle\} \quad \text{(A16)}$$

This equation means that the magnetic interaction between the monomer units in the dimer can be estimated from the difference of the spin splitting of the POMO between the dimer and the

monomer. Therefore, the magnetic interaction of the dimer $J_{A-B}$ is written as

$$J_{A-B} = \Sigma_{\zeta} (\Delta\epsilon_{A-B,\zeta}^{\uparrow\downarrow} - \Delta\epsilon_{A,l}^{\uparrow\downarrow\circ}) \qquad \text{(A17)}$$

where the summation is of all the POMOs.

## References and Notes


(1) (a) Kahn, O.; Pei, Y.; Verdaguer, M.; Renard, J. P.; Sletten, J. *J. Am. Chem. Soc.* **1988**, *110*, 782. (b) Kahn, O. *Angew. Chem., Int. Ed. Engl.* **1985**, *24*, 834.

(2) (a) Caneschi, A.; Gatteschi, D.; Renard, J. P.; Rey, P.; Sessoli, R. *Inorg. Chem*. **1989**, *28*, 3314. (b) Caneschi, A.; Gatteschi, D.; Renard, J. P.; Rey, P.; Sessoli, R. *Inorg. Chem*. **1989**, *28*, 1976. (c) Caneschi, A.; Gatteschi, D.; Sessoli, R.; Rey, P. *Acc. Chem. Res*. **1989**, *22*, 392.

(3) Inoue, K.; Iwamura, H. *J. Am. Chem. Soc*. **1994**, *116*, 3173.

(4) Tamaki, H; Zhong, Z. J.; Matsumoto, N.; Kida, S.; Koikawa, M.; Achiwa, N.; Hashimoto, Y.; Okawa, H. *J. Am. Chem. Soc*. **1992**, *114*, 6974. Decurtins, S.; Schmalle, H. W.; Schneuwly, P.; Ensling, J.; Gütlich, P. *J. Am. Chem. Soc.* **1994**, *116*, 9521.

(5) McConnell, H. M. *Proc. Robert A. Welch Found. Conf. Chem. Res*. **1967**, *11*, 144.

(6) (a) Miller, J. S.; Calabrese, J. C.; Rommelmann, H.; Chittipeddi, S. R.; Zhang, J. H.; Reiff, W. M.; Epstein, A. J. *J. Am. Chem. Soc*. **1987**, *109*, 769. (b) Manriquez, J. M.; Yee, G. T.; McLean, R. S.; Epstein, A. J.; Miller, J. S. *Science* **1991**, *252*, 1415.

(7) Oshio, H. *Inorg. Chem.* **1993**, *32*, 4213. Oshio, H.; Ino, E.; Mogi, I.; Ito, T. *Inorg. Chem*. **1993**, *32*, 5697.

(8) For example see: Yoshizawa, K.; Hoffmann, R. *J. Am. Chem. Soc*. **1995**, *117*, 6921.

(9) Bekaroglu, Ö.; Sarisaban, S.; Koray, A. R.; Ziegler, M. L. *Z. Naturforsch*. **1977**, *B32*, 387.

(10) (a) Endres, H.; Jannack, T.; Prickner, B. *Acta Crystallogr*. **1980**, *B36*, 2230. (b) Herbstein, F. H.; Marsh, R. E. *Acta Crystallogr*. **1982**, *B38*, 1051.

(11) Endres, H.; Genc. N.; Nöthe, D. *Acta Crystallogr*. **1983**, *C39*, 701.

(12) Hirotsu, T.; Takagi, N.; Sakakibara, J.; Katoh, S.; Senô, M. *J. Chem. Soc., Chem. Commun.* **1990**, 1631.

(13) Averill, F. W.; Ellis, D. E. *J. Chem. Phys*. **1973**, *59*, 6412. Ellis, D. E.; Adachi, H.; Averill, F. W. *Surf. Sci*. **1976**, *58*, 497. Rosen, A.; Ellis, D. E.; Adachi, H.; Averill, F. W. *J. Chem. Phys.* **1976**, *65*, 3629. Adachi, H.; Tsukada, M.; Satoko, C. *J. Phys. Soc. Jpn.* **1978**, *45*, 875. Adachi, H.; Shiokawa, S.; Tsukada, M.; Satoko, C.; Sugano, S. *J. Phys. Soc. Jpn.* **1979**, *47*, 1528.

(14) Fischer, E. *Ber*. **1889**, *22*, 1930. Pearse, G. A., Jr.; Pflaum, R. T. *Anal. Chem.* **1960**, *32*, 213.

(15) The Chemical Society of Japan, Ed. *Kagaku Binran-Kisohen II*; Maruzen: Tokyo, 1984; p. II-508 (Japanese).

(16) The program of the DV-Xα method was offered from Prof. H. Adachi (Kyoto University).

(17) Baker, G. A., Jr.; Rushbrooke, G. S.; Gilbert, H. E. *Phys. Rev. A* **1964**, *135*, 1272.

(18) Swank, D. D.; Landee, C. P.; Willet, R. D. *Phys. Rev. B* **1979**, *20*, 2154.

(19) Leggett, D. J. The Determination of Formation Constants-An Overview of Computational Methods for Data Processing. In *Computaional Methods for the Determination of Formation Constants*; Leggett, D. J., Ed.; Plenum Press: New York, 1985; pp 5−9.

(20) This calculated value is compensated by the contribution from Schiff bases.

(21) For example see: Lubitz, W.; Winscom, C. J.; Diegruber, H.; Moseler, R. *Z. Naturforsch*. **1987**, *A42*, 970.

(22) Kahn, O.; Sikorav, S.; Gouteron, J.; Jeannin, S.; Jeannin, Y. *Inorg. Chem.* **1983**, *22*, 2877. Caneschi, A.; Gatteschi, D.; Sessoli, R. *Inorg. Chem.* **1993**, *32*, 4612.

(23) The $75a_g^{\uparrow}$ and $75a_u^{\uparrow}$ of $2CoL_2$ can be approximately expressed with the $38a_g^{\uparrow}$ of $CoL_2$ in the similar manner.

(24) The $76a_g^{\downarrow}$ and $76a_u^{\downarrow}$ of $2CuL_2$ can be approximately expressed by use of the $39a_g^{\downarrow}$ of $CuL_2$ in the similar manner.

(25) Kahn, O.; Briat, B. *J. Chem. Soc., Perkin Trans. 2* **1976**, *72*, 268. Girerd, J. -J.; Charlot, M. -F.; Kahn, O. *Mol. Phys*. **1977**, *34*, 1063. Tola, P.; Kahn, O.; Chauvel, C.; Coudanne, H. *Nouv. J. Chim.* **1977**, *1*, 467.

(26) Slater, J. C. *The Calculation of Molecular Orbitals*; Wiley: New York, 1979; p 8.